Effects of Blockage in Deploying mmWave Drone Base Stations for 5G Networks and Beyond

Margarita Gapeyenko†, Irem Bor-Yaliniz⋆, Sergey Andreev†, Halim Yanikomeroglu⋆, and Yevgeni Koucheryavy†
†Tampere University of Technology, Tampere, Finland
⋆Carleton University, Ottawa, Canada

Invited Paper

***Abstract*—Due to their unconstrained mobility and capability to carry goods or equipment, *unmanned aerial vehicles* (UAVs) or *drones* are considered as a part of the fifth-generation (5G) wireless networks and become attractive candidates to carry a base station (BS). As 5G requirements apply to a broad range of uses cases, it is of particular importance to satisfy those during *spontaneous and temporary events*, such as a marathon or a rural fair. To be able to support these scenarios, mobile operators need to deploy significant radio access resources quickly and on demand. Accordingly, by focusing on 5G cellular networks, we investigate the use of drone-assisted communication, where a drone is equipped with a millimeter-wave (mmWave) BS. Being a key technology for 5G, mmWave is able to facilitate the provisioning of the desired per-user data rates as drones arrive at the service area whenever needed. Therefore, in order to maximize the benefits of *mmWave-drone-BS* utilization, this paper proposes a methodology for its optimized deployment, which delivers the optimal height, coordinates, and coverage radius of the drone-BS by taking into account the *human body blockage* effects over a mmWave-specific channel model. Moreover, our methodology is able to maximize the number of offloaded users by satisfying the target signal quality at the cell edge and considering the maximum service capacity of the drone-BS. It was observed that the mmWave-specific features are extremely important to consider when targeting efficient drone-BS utilization and thus should be carefully incorporated into analysis.**

***Index Terms*—5G networks and beyond; mmWave; human body blockage; network slicing; drone-cell communications.**

I. Introduction and motivation

The recent developments in *unmanned aerial vehicles* (UAVs) attracted an increased attention from the wireless communications community. It is envisioned that UAVs are about to become a part of the fifth generation (5G) of wireless networks [1]. One of the emerging applications is the use of the UAVs equipped with wireless transceivers, or *drone base stations* (BSs), which have been proposed to improve the connectivity levels in 5G systems and beyond [2]. In particular, latest research illustrates that autonomous flying robots become an attractive solution to boost network capacity on demand, which is particularly desirable for spontaneous and temporary events, such as rural fair [3] or marathon use cases [4]. This paper specifically argues for the use of drones enhanced with high-rate millimeter-wave (mmWave) radio technology to support these scenarios.

While an autonomous fleet of drones flying around the city [5] may still be a futuristic concept, the utilization of several specialized drones operating under human control is possible from an engineering perspective already today [6], [7]. At the same time, the use of drone-BSs introduces new challenges, such as extra operating costs, endurance, and backhauling [2], [8]. In order to seamlessly integrate drone-BSs into the 5G system architecture, a new concept named network slicing might become an appropriate candidate [2]. Slicing can facilitate the integration of aerial BSs with the terrestrial network by providing a slice with the necessary fronthaul, backhaul, and network functions by also considering mobility of the drone-BS. Smart integration of drones into the 5G infrastructure additionally requires efficient drone placement mechanisms to improve the overall system performance.

Despite a number of research works on drone deployment [9]–[11], the specifics of mmWave-based drone-assisted communication has remained insufficiently studied so far. Operating in extremely high frequency (EHF) bands and having larger bandwidths at its disposal, mmWave radio technology is being shaped as the 5G New Radio [12]. Along with their benefits, mmWave systems are facing many challenges. One of these is shorter wavelengths for which smaller objects, such as humans, become obstacles for the line-of-sight (LoS) radio propagation [13], [14]. Hence, it is crucial to account for the *human body blockage* when evaluating the performance or planning the deployment of mmWave-BSs. In contrast to lower frequencies, another challenge at mmWave bands is that the path loss (PL) increases significantly with the growing distance from a transmitter (Tx) to a receiver (Rx) [15]. Hence, there is a trade-off between placing a drone at a higher altitude (which would provide better LoS links) and keeping the PL minimal (which increases with the growing distance).

There are several important benefits that motivate the utilization of mmWave-based drone-BSs, particularly for the temporary and spontaneous events, as described below:

- Able to arrive at the crowded location quickly, drones equipped with wireless access capabilities help operators serve events, where traffic demand becomes higher than expected for a certain period of time, but where it is not feasible to deploy a static network infrastructure to serve such amounts of data on a regular basis.
- Even though higher altitudes lead to larger probabilities to maintain the LoS link, they also increase the three-dimensional (3D) distance, thus making the PL higher. Therefore, the optimal altitude may exist. While the terrestrial infrastructure cannot alter the height of the BSs quickly in order to improve the signal quality, the flexibility of the drone-BSs offers an opportunity to place them over the crowd and adjust their height when needed.

- To achieve 100 Mbit/s per user expected of the 5G systems, mmWave communication is an appropriate solution whereas the conventional infrastructure will need a significant number of cellular BSs to support the required data rate, which leads to severe interference. The latter could be shown using simple analysis where the link capacity for the cell edge-user over mmWave with the carrier of 28 GHz and the conventional microwave cellular link with the carrier of 2.1 GHz is calculated as $r(x) = B_u \log[1 + S(x)]$. Here, B_u is the bandwidth available to the user of interest and $S(x)$ is the average signal-to-noise ratio (SNR) for this user at the cell edge of radius x. For the same number of active users, the cellular link with the maximum available bandwidth (B) of 20 MHz delivers about 10 times lower data rates than what mmWave (B = 1 GHz) does, even in ideal conditions where no interference is assumed. In an optimistic case, to provide the average data rate of 100 Mbit/s per user, for a cell having 50 m radius and 70 users, one mmWave-BS is sufficient, whereas the required number of the conventional BSs is 10 times higher. Therefore, the larger bandwidth of mmWave-BSs accentuates the utilization of those to support the mass events and mitigate the growth of interference to deliver the 5G date rates [16].

All of the above motivates the need for efficient placement of mmWave-drone-BSs to provide with a better link quality and benefit from the maximum number of users offloaded from the cellular infrastructure, where the main features of mmWave communication would be considered. In this paper, we investigate efficient deployment of a mmWave-drone-BS by taking into account the properties of mmWave communication, where the LoS link may be blocked by a human body. Having in mind that the height of the mmWave-drone-BS is comparable with the height of the BSs mounted on the walls of the buildings and assuming quasi-stationary drones hovering at a certain altitude [17], we approximate the air-to-ground channel model with the terrestrial channel model [18] for the sake of our first-order analysis.

The main contributions of this paper are as follows.

- By adopting a terrestrial mmWave channel model for the air-to-ground mmWave communication as well as by accounting for the human body blockage, we derive the optimal height of the drone-BS.
- By assuming a Poisson distribution of user locations for the adopted mmWave PL model, we formulate and solve a 3D placement problem. The latter produces the optimal height and horizontal location for the drone-BS as well as the cell radius. Our theoretical results for the optimal height demonstrate a tight match with those obtained by solving the 3D placement problem.

The rest of this text is organized as follows. In Section II, we introduce our system model with its main assumptions. Then, the proposed optimization methodology is described in Section III. The numerical results are offered in Section IV. Conclusions are drawn in the last section.

II. System model

Our example rural-fair scenario considers a set of identical users, $\mathbb{M}$, which are distributed randomly in the area of interest as illustrated in Fig. 1. We assume that the existing operator's infrastructure is not planned for such a spontaneous and temporary mass event. Therefore, the operator is incapable of serving all the users at the fair. Hence, we consider the assistance of a mmWave-drone-BS to inject capacity across space and time. The mmWave-drone-BS is integrated into the current infrastructure via a dedicated long range backhaul channel over a different frequency [19].

Inspired by the adoption of terrestrial channel models for air-to-ground channels of quasi-stationary drone-BSs [9], [10], [17], we employ the model in [20] for the first-order analysis of mmWave-drone-BSs. There are two motivations for choosing a terrestrial channel model. First, contemporary drone-BSs with a rotary wing [21] can be made as stationary as cell towers, especially under mild weather conditions. Second, the short range of mmWave links prevents from using high-altitude drones due to the inherently high PL with increasing distance between the Tx and Rx. Therefore, the altitude of a mmWave-drone-BS must be comparable with the altitude of the static mmWave-BSs deployed on the walls, lamp posts, etc. For the sake of our analysis, the small scale fluctuations in the environment are neglected as proposed in [17].

The considered scenario consists of the mmWave-drone-BS located at height h_D and human blockers modeled as cylinders with the average height of h_B and the average diameter of g_B. For a snapshot analysis, assume a Poisson field of static human blockers with the density of λ, where $|\mathbb{M}|$ humans are distributed across the area S with the parameter λS, and $|\cdot|$ indicates the cardinality of a set. Note that all users are considered as blockers for each other. The user terminal is assumed to be located at the height h_R, where $h_R < h_B$, since the terminal carried by a human is usually lower than the height of the human itself. Hence, if the user i is communicating with the mmWave-drone-BS, then all other users/humans in the coverage area $\mathcal{A}$ with radius R are blockers, if their heights are large enough to block the LoS

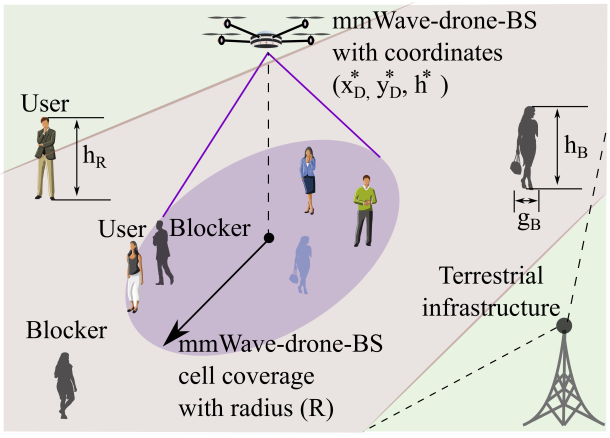

Fig. 1. Target scenario with mmWave-drone-BS, users, and blockers.

TABLE I
NOTATION AND PARAMETERS

Parameter	Description
S	Area of interest
h_D, h_R, h_B	Height of drone-BS, Rx, and human blockers
R	Cell radius of the drone-BS
d_i, r_i	3D, 2D distance between drone-BS and i^{th} Rx
g_B	Diameter of human blockers
λ	Density of human blockers
$\mathbb{P}_L$	Probability of LoS
$L_{L,i}$, $L_{N,i}$	Path loss for LoS/nLoS i^{th} Rx
$L_{a,i}$	Average path loss for i^{th} Rx
$\lvert\mathbb{M}\rvert$	Total number of humans in the area of interest
h^*	Optimal height of the drone-BS
$({x_D}^*, {y_D}^*)$	Optimal 2D position of the drone-BS
N	Maximum number of users served by one drone-BS
Q, σ_i	Target SNR, SNR for i^{th} Rx
γ	Maximum tolerable path loss

between Rx and Tx. Note that the coverage radius R depends on the ability of drone-BS to support on average the minimum quality-of-service (QoS) experienced by the cell edge user; therefore, it is highly affected by the height of the drone-BS and the probability of LoS as will be shown later.

Following [22], we assume that radio interference does not have a major effect, which is a common assumption for most mmWave-based systems with highly directional antennas, and that the system under study is *noise-limited*.

Recall that the PL models for LoS and nLoS links at mmWave frequencies follow [18] and are given as

$$\begin{aligned} L_{L,i} &= \alpha_L + 10\beta_L \log_{10}(d_i), \\ L_{N,i} &= \alpha_N + 10\beta_N \log_{10}(d_i), \end{aligned} \tag{1}$$

where α_L, β_L, α_N, and β_N are the parameters of the LoS and nLoS PL models, and $d_i = \sqrt{(x_i - x_D)^2 + (y_i - y_D)^2 + (h_D - h_R)^2}$ is the 3D distance between the drone-BS and Rx.

In order to account for the human body blockage, we adopt the probability of LoS, $\mathbb{P}_L$, for a user i from [20] by modifying it in the case of the constant height and diameter of blockers for further analytic tractability as

$$\mathbb{P}_L(r_i, h_D) = \exp\left(- \lambda g_B \frac{r_i(h_B - h_R)}{(h_D - h_R)} \right), \tag{2}$$

where r_i is 2D distance between drone-BS and Rx.

Then, the average PL for the cell edge user i, located at distance R from Tx, becomes

$$L_{a,i} = \mathbb{P}_L(R, h_D) L_{L,i} + \left[1 - \mathbb{P}_L(R, h_D)\right] L_{N,i}. \tag{3}$$

As one may find in [17] and similar works, the average value of PL is sufficient to perform the first-order analysis. Since the random behavior with the corresponding distribution is not the focus of this study, the distributions of fading and shadowing are disregarded. As it was observed in [20], there exists the optimal height of the Tx, where the average PL assumes its minimum value.

III. MMWAVE-DRONE-BS DEPLOYMENT

In order to support the current cellular infrastructure and provide higher data rates for every user in the area, the aim is to offload as many users as possible to the mmWave-drone-BS. Because the users are randomly distributed in the region, the area to be covered by a mmWave-drone-BS (drone-cell coverage) and the altitude of the drone-BS are not known a priori.

On the one hand, deploying a mmWave-drone-BSs at a higher altitude leads to the greater LoS probability as can be observed from (2). On the other hand, mmWave-drone-BSs are energy critical devices and higher altitudes may require more transmission power due to increased distance between the users and the drone-BSs to compensate for larger PL. Therefore, the objective of covering the maximum number of users with minimum energy means the smallest area enclosing the highest number of users, while the minimum height that can provide coverage over that area must be derived.

As observed in (2) and (3), the average PL depends on the altitude of the Tx, as well as the horizontal distance between the Tx and Rx. Therefore, the optimal placement of a mmWave-drone-BS involves all dimensions, namely, the optimal position is $({x_D}^*, {y_D}^*, h^*)$. Fixing the horizontal location of the drone-BS and searching for h^* to provide the maximum number of users to be covered (*1D search*), or fixing the altitude and searching for $({x_D}^*, {y_D}^*)$ (*2D search*) may not result in the most effective deployment. The search for the optimal position of a mmWave-drone-BS must thus be performed in 3D. Not only the expansion of the search space to 3D makes it very hard to conduct an exhaustive search, but also (3) is analytically difficult. Therefore, in this section, we propose an efficient 3D placement method for mmWave-drone-BSs.

The problem to find (x_D^*, y_D^*, h^*) can be formulated as

$$\underset{x_D, y_D, h, \{m_i\}}{\text{maximize}} \quad \sum_{i \in \mathbb{M}} m_i \tag{4a}$$

subject to

$$m_i \sigma_i \geq m_i Q, \qquad \forall i = 1, ..., |\mathbb{M}|, \tag{4b}$$

$$\sum_{i \in \mathbb{M}} m_i \leq N, \qquad \forall i = 1, ..., |\mathbb{M}|, \tag{4c}$$

$$x_l \leq x_D \leq x_u, \tag{4d}$$

$$y_l \leq y_D \leq y_u, \tag{4e}$$

$$h_l \leq h \leq h_u, \tag{4f}$$

$$m_i \in \{0, 1\}, \qquad \forall i = 1, ..., |\mathbb{M}|, \tag{4g}$$

where m_i is a binary variable indicating whether the i^{th} user of the set $\mathbb{M}$ is covered (1) or not (0), x_D, y_D are the possible coordinates of the drone-BS, $h = h_D - h_R$, and σ_i is the SNR for the user i. Then, Q and N represent the target SNR level for the served user i and the capacity of the drone-BS in terms of the maximum number of users that it can serve, respectively. The upper and the lower limits of the available positions across all three dimensions are indicated by the subscripts u and l,

correspondingly. While (4b) determines which users can be served, (4c) captures the maximum number of the served users.

Apart from the antenna gains, transmit power, etc., the maximum tolerable PL for the i^{th} user, γ, corresponds to the target SNR of the i^{th} user, Q. Hence, using (3), (4b) becomes $m_i L_{a,i} \leq \gamma$. Note that our approach is not limited to the model in [18], and other channel models may be considered as well. After further derivations, the QoS depicted in (4b) can be represented in terms of distance between user i and the drone-BS as

$$r_i^2 + h^2 \leq 10^{[2\tilde{\gamma}+\mathbb{P}_L(R,h)k_2]/[\mathbb{P}_L(R,h)k_3+k_4]}, \tag{5}$$

where $r_i = \sqrt{(x_i - x_D)^2 + (y_i - y_D)^2}$ is 2D distance between user i and the drone-BS, $\tilde{\gamma} = \gamma - \alpha_N$, $k_2 = \alpha_N - \alpha_L$, $k_3 = 10(\beta_L - \beta_N)$, $k_4 = 10\beta_N$, whereas R is the coverage radius of the drone-BS. Note that any user with the horizontal distance of less than R will be served, since its minimum SNR requirements at the cell edge are satisfied on average. Furthermore, introducing the variable $\omega = R/h$ and expressing $\mathbb{P}_L(R,h)$ in terms of ω, (4b) becomes

$$r_i^2 \leq \Gamma(\omega), \tag{6}$$

where $\Gamma(\omega)$ is the following

$$\Gamma(\omega) = \frac{10^{(2\tilde{\gamma}+k_2 \mathrm{e}^{\omega k_1})/(k_3 \mathrm{e}^{\omega k_1}+k_4)}}{1+\frac{1}{\omega^2}}, \tag{7}$$

where $k_1 = -\lambda g_B (h_B - h_R)$, $h_B > h_R$.

Proposition 1. *The function $\Gamma(\omega)$ has the maximum point ω^*, which is considered to be optimal.*

Proof. To find the maximum point, we first need to establish an extremum point of $\Gamma(\omega)$, by taking a derivative, equating it to zero, and solving the following

$$\begin{aligned} &k_1 e^{\omega k_1}(\omega^3 + \omega)(k_2 k_4 - k_3\tilde{\gamma})\ln(10) \\ &+ (e^{\omega k_1} k_3 + k_4)^2 = 0. \end{aligned} \tag{8}$$

Note that the above always has a solution for $\beta_L < \beta_N$ and $h_B > h_R$. It could be solved numerically and offers the extremum point, ω^*. By taking the second derivative of (8) and obtaining the negative value at the extremum point ω^*, we establish that ω^* is also the maximum of $\Gamma(\omega)$.

As there is no closed form solution to find ω^*, it is important to show the uniqueness of this point, which is formally proven in Appendix. □

The optimal value, $\Gamma(\omega^*)$, can be inserted into (6). The resulting optimization problem is then

$$\underset{x_D, y_D, \{m_i\}}{\text{maximize}} \quad \sum_{i \in \mathbb{M}} m_i \tag{9a}$$

subject to

$$r_i \leq \sqrt{\Gamma(\omega^*)} + K(1 - m_i), \ \forall i = 1, ..., |\mathbb{M}|, \tag{9b}$$

$$x_l \leq x_D \leq x_u, \tag{9c}$$

$$y_l \leq y_D \leq y_u, \tag{9d}$$

$$m_i \in \{0, 1\}, \qquad \forall i = 1, ..., |\mathbb{M}|, \tag{9e}$$

where K is a large enough value [9]. Once x_D^* and y_D^* are obtained, R can be calculated by identifying the user at the drone-cell edge, i.e., $\max_{m_i \in \mathbb{M}} (r_i | m_i = 1)$. Then, h^* can be derived by using ω^*.

Moreover, the optimal height can also be produced directly from (3) by taking a derivative of the average PL. Note that in this case, the cell coverage R should be known beforehand. In this paper, we propose an approach to numerically establish the optimal height of Tx, h^*, by solving the following

$$\begin{aligned} &- C\big[\alpha_L - \alpha_N\big]\big[(h^* - h_R)^2 + R^2\big] e^{\frac{C}{h^* - h_R}} \\ &+ 10C\big[\beta_N - \beta_L\big] \log_{10}\left(\sqrt{(h^* - h_R)^2 + R^2}\right) \\ &+ \frac{10\big[\beta_L - \beta_N\big]\big[h^* - h_R\big]^3}{\ln(10)} e^{\frac{C}{h^* - h_R}} + 10\beta_N = 0, \end{aligned} \tag{10}$$

where the auxiliary variable $C = -\lambda g_B R(h_D - h_R)$.

The above 3D placement problem can be solved by using e.g., interior-point optimization method via MOSEK [23], both efficiently and accurately. Indeed, the efficient 3D placement algorithm in (9a) offers the same result as in (10) for the same value of R derived with our 3D placement algorithm.

IV. Numerical results and discussion

In this section, we illustrate representative numerical results produced for different human densities λ, where the humans are uniformly distributed within a 100x100 m^2 area. The parameters for the considered scenario are collected in Table II. Our target is to serve the maximum number of users from the set of total number of humans $|\mathbb{M}|$ with a mmWave-drone-BS. It should be noted that for every realization of the scenario the coordinates of the users as well as the total number $|\mathbb{M}|$ are known for the problem to solve. We set the maximum tolerable path loss, γ, equal to 110 dB based on the following assumed parameters: bandwidth is 1 GHz, Rx and Tx antenna gains are 5 dB and 10 dB, respectively, Tx power is 20 dBm, noise figure is 6 dB, and target SNR is 3 dB. Also, 95% confidence interval is calculated for the entire set of runs to demonstrate the consistency of the proposed method. The following formula is used for confidence interval calculations: $\bar{x} \pm \mathrm{Z}_{a/2} \times \frac{\sigma}{\sqrt{(n)}}$, where $\bar{x}$ is the mean, Z is the confidence coefficient, a denotes the confidence interval, while σ and n represent the standard deviation and the sample size, respectively.

First, Fig. 2 demonstrates the behavior of the altitude of the mmWave-drone-BS as the density of blockers increases.

TABLE II
Baseline system parameters

Parameter	Value
Height of Rx, h_R	1.3 m
Height of a human blocker, h_B	1.7 m
Diameter of a human blocker, g_m	0.5 m
Frequency band	28 GHz
LoS path loss model parameters	$\alpha_L = 61.4$, $\beta_L = 2$
nLoS path loss model parameters	$\alpha_N = 72$, $\beta_N = 2.92$
Maximum number of users served by drone-BS, N	100
Area of interest, S	100x100 m^2

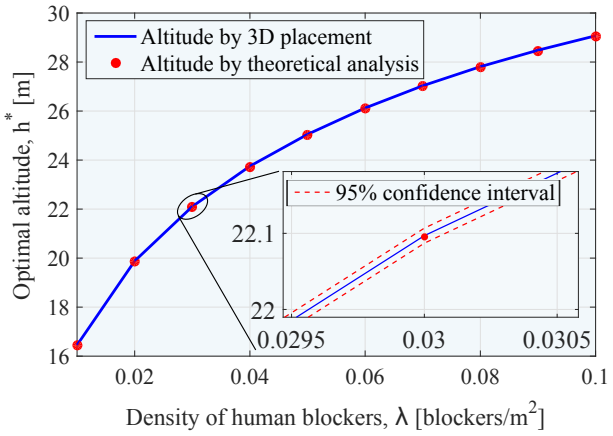

Fig. 2. Comparison of the optimal altitude results from 3D placement with theoretical analysis vs. density of blockers, λ.

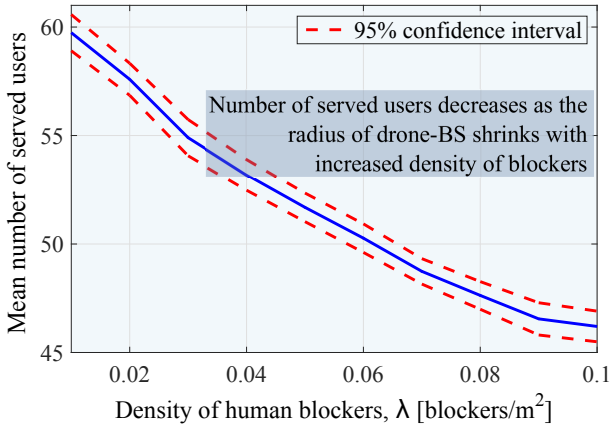

Fig. 4. Number of users served by mmWave-drone-BS vs. density of blockers, λ.

We observe that the altitude becomes higher as the density grows. The reason is that higher altitude makes the probability of blockage lower but sacrifices the radius of the drone-BS coverage in order to reduce the 3D distance, in order to satisfy the minimum SNR. This confirms the importance of appropriate height selection. In addition, the plot shows a comparison of the altitude by the 3D placement with that derived from the theoretical result in (10). The analysis requires the cell coverage obtained with the 3D placement in order to produce the height of the BS. The results indicate a reasonable match between the two. It should be noted that the proposed 3D placement provides the coordinates of the drone-BS, not only altitude but also the location in the horizontal plane, which allows for efficient drone-cell deployment in order to serve the maximum number of users.

In Fig. 3, the aforementioned relation between the mean value of the mmWave-drone-BS cell coverage and the density of blockers is displayed. It is observed that the cell radius, R, decreases as the density grows. This could be explained by the fact that the probability of blockage becomes larger, thus yielding a higher altitude of the drone-BS and smaller cell radius to reduce 3D distance in order to facilitate the satisfaction of the minimum SNR requirements.

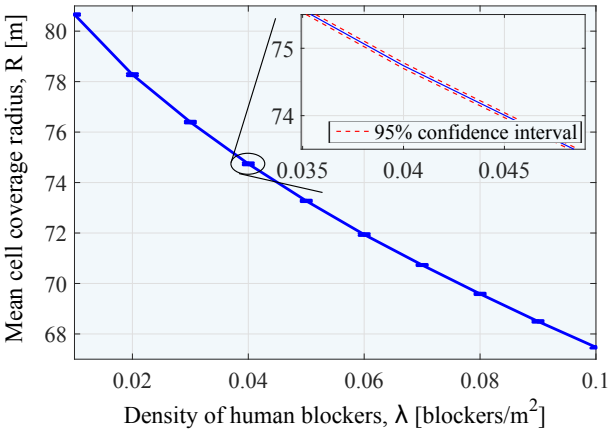

Fig. 3. Radius, R, (m) vs. density of blockers, λ, with error bar.

Further, we consider the number of served users as illustrated in Fig. 4. We learn that the average number of users served by one drone-BS decreases as the density of blockers grows. This could be explained by the fact that the effective cell radius degrades as it was shown earlier. Therefore, the density of blockers highly affects the optimal height of the drone-BS, which then impacts the shrinking of the cell coverage, and finally the reduced number of served users. This implies the importance of considering all of the variables as they have a major effect on the load of the BS as well as its ability to satisfy the minimum QoS requirements.

V. Conclusion and Future Work

Drone-assisted cellular communication is currently attracting significant research attention from both academia and industry by becoming a new frontier in 5G wireless networks and beyond. While mmWave radio systems are expected to deliver the required 100 Mbit/s of user experienced data rate, there still remains a question of how to boost cell capacity quickly and on-demand, which is highly relevant for spontaneous and temporary events, such as open-air festivals in rural areas or marathons [4]. To ensure efficient support of these emerging scenarios, we advocate for the use of mmWave-drone-BSs.

Despite a number of past papers on drone-BS placement, the specifics of mmWave communication, including LoS blockage by human bodies, has not been taken into consideration before. In this paper, we study the effective deployment of a mmWave-drone-BS as well as derive the corresponding height and cell radius. Further, we produce an analytical result for the optimal height of Tx. We thus observe that the density of blockers has a dramatic effect on the desired height, the coverage radius, and the number of served users. Furthermore, an increase in the density of blockers leads to a sharp drop in the total number of users that could be served satisfactorily. Therefore, our future work is to consider the effects related to multiple drone-BSs and their needed densities in order to serve all of the users.

APPENDIX

In order to demonstrate the uniqueness of the maximum point ω^*, we prove that the $\Gamma(\omega)$ function is quasiconcave by following the definition [24]

$$\Gamma\big(\lambda_C x + [1-\lambda_C]y\big) \geq \min\{\Gamma(x), \Gamma(y)\}, \tag{11}$$

where $\lambda_C \in [0,1]$, $x, y \in S_C$, and $S_C \to \mathbb{R}$.

Assume that $x < y$, then (11) could be written as

$$\frac{10^{\frac{2\bar{\gamma}+k_2\exp\left(k_1(\lambda_C x+[1-\lambda_C]y)\right)}{k_3\exp\left(k_1(\lambda_C x+[1-\lambda_C]y)\right)+k_4}}}{1+\frac{1}{(\lambda_C x+(1-\lambda_C)y)^2}} \geq \frac{10^{\frac{2\bar{\gamma}+k_2\exp(zk_1)}{k_3\exp(zk_1)+k_4}}}{1+\frac{1}{z^2}}, \tag{12}$$

where z is equal to x or y depending on the minimum value of Γ.

It is easy to see that by transferring the right part to the left side of (12) and reducing to a common denominator, the last one is always greater than 0. Therefore, to make the overall expression be greater than 0, one should prove the positive sign of the numerator.

Let $A = \frac{2\bar{\gamma}+k_2\exp\left(k_1(\lambda_C x+[1-\lambda_C]y)\right)}{k_3\exp\left(k_1(\lambda_C x+[1-\lambda_C]y)\right)+k_4}$ and $B = \frac{2\bar{\gamma}+k_2\exp(zk_1)}{k_3\exp(zk_1)+k_4}$, then the numerator of (12) becomes

$$10^A\left(1+\frac{1}{z^2}\right) - 10^B\left(1+\frac{1}{\big(\lambda_C x+[1-\lambda_C]y\big)^2}\right) \geq 0. \tag{13}$$

Note that $\Gamma(\omega)$ for $\omega \in (0, \omega^*)$ is increasing; therefore, (12) is always true.

After further derivations, it could be shown that $A \geq B$ for $z = y$. The calculations are omitted here due to a large number of simple algebraic transformations. When $\min\{\Gamma(x), \Gamma(y)\} = \Gamma(y)$, $z = y$, (13) takes the form of

$$10^A + \frac{10^A}{y^2} - 10^B - \frac{10^B}{\big(\lambda_C x+[1-\lambda_C]y\big)^2} \geq 0. \tag{14}$$

Finally, it is easy to see that $(10^A - 10^B) \geq 0$ and $\big(\frac{10^A}{y^2} - \frac{10^B}{(\lambda_C x+[1-\lambda_C]y)^2}\big) \leq (10^A - 10^B)$ in (14). Therefore, (12) holds for $z = y$ as well.

Therefore, ω^* is a maximum point of Γ, [24].

ACKNOWLEDGMENTS

This work was funded in part by the Academy of Finland (project PRISMA) and in part by Huawei Canada Co., Ltd. The work of M. Gapeyenko was supported by the Nokia Foundation.

REFERENCES

[1] 3GPP, "Study on scenarios and requirements for next generation access technologies (Release 14)," 3GPP TR 38.913 V14.3.0, August 2017.

[2] I. Bor-Yaliniz and H. Yanikomeroglu, "The new frontier in RAN heterogeneity: Multi-tier drone-cells," *IEEE Communications Magazine Special Issue on 5G Radio Access Network Architecture and Technologies*, vol. 54, no. 11, pp. 48–55, November 2016.

[3] Z. Xiao, P. Xia, and X. Xia, "Enabling UAV cellular with millimeter-wave communication: potentials and approaches," *IEEE Communications Magazine*, vol. 54, no. 5, pp. 66 – 73, May 2016.

[4] METIS, "Updated scenarios, requirements and KPIs for 5G mobile and wireless system with recommendations for future investigations," Deliverable D1.5, April 2015.

[5] I. Bekmezci, O. K. Sahingoz, and S. Temel, "Flying ad hoc networks (FANETs): A survey," *Ad Hoc Networks*, vol. 11, no. 3, pp. 1254–1270, May 2013.

[6] S. Chandrasekharan, K. Gomez, A. Al-Hourani, S. Kandeepan, T. Rasheed, L. Goratti, L. Reynaud, D. Grace, I. Bucaille, T. Wirth, and S. Allsopp, "Designing and implementing future aerial communication networks," *IEEE Communications Magazine*, vol. 54, no. 5, pp. 26–34, May 2016.

[7] D. Solomitckii, M. Gapeyenko, V. Semkin, S. Andreev, and Y. Koucheryavy, "Technologies for efficient amateur drone detection in 5G millimeter-wave cellular infrastructure," *IEEE Communications Magazine*, vol. 56, no. 1, pp. 43–50, January 2018.

[8] E. Kalantari, M. Z. Shakir, H. Yanikomeroglu, and A. Yongacoglu, "Backhaul-aware robust 3D drone placement in 5G+ wireless networks," in *IEEE International Conference on Communications Workshops (ICC Wkshps)*, May 2017.

[9] I. Bor-Yaliniz, A. El-Keyi, and H. Yanikomeroglu, "Efficient 3-D placement of an aerial base station in next generation cellular networks," in *2016 IEEE International Conference on Communications*, May 2016.

[10] M. Mozaffari, W. Saad, M. Bennis, and M. Debbah, "Drone small cells in the clouds: Design, deployment and performance analysis," in *IEEE Global Communications Conference (GLOBECOM)*, December 2015.

[11] ——, "Efficient deployment of multiple unmanned aerial vehicles for optimal wireless coverage," *IEEE Communications Letters*, vol. 20, no. 8, pp. 1647–1650, August 2016.

[12] J. G. Andrews, S. Buzzi, C. Wan, S. V. Hanly, A. Lozano, A. C. K. Soong, and J. C. Zhang, "What will 5G be?" *IEEE Journal on Selected Areas in Communications*, vol. 32, no. 6, pp. 1065–1082, June 2014.

[13] M. Abouelseoud and G. Charlton, "The effect of human blockage on the performance of millimeter-wave access link for outdoor coverage," in *IEEE 77th Vehicular Technology Conference*, June 2013.

[14] M. Gapeyenko, A. Samuylov, M. Gerasimenko, D. Moltchanov, S. Singh, M. R. Akdeniz, E. Aryafar, N. Himayat, S. Andreev, and Y. Koucheryavy, "On the temporal effects of mobile blockers in urban millimeter-wave cellular scenarios," *IEEE Transactions on Vehicular Technology*, vol. 66, no. 11, pp. 10 124–10 138, November 2017.

[15] S. Sun, T. Rappaport, T. A. Thomas, A. Ghosh, H. C. Nguyen, I. Z. Kovacs, I. Rodriguez, O. Koymen, and A. Partyka, "Investigation of prediction accuracy, sensitivity, and parameter stability of large-scale propagation path loss models for 5G wireless communications," *IEEE Transactions on Vehicular Technology*, vol. 65, no. 5, pp. 2843–2860, May 2016.

[16] 3GPP, "Study on channel model for frequencies from 0.5 to 100 GHz (Release 14)," 3GPP TR 38.901 V14.3.0, January 2018.

[17] A. Al-Hourani, S. Kandeepan, and S. Lardner, "Optimal LAP altitude for maximum coverage," *IEEE Wireless Communications Letters*, vol. 3, no. 6, pp. 569–572, December 2014.

[18] M. R. Akdeniz, Y. Liu, M. K. Samimi, S. Sun, S. Rangan, T. S. Rappaport, and E. Erkip, "Millimeter wave channel modeling and cellular capacity evaluation," *IEEE Journal on Selected Areas in Communications*, vol. 32, no. 6, pp. 1164–1179, June 2014.

[19] S. Hur, T. Kim, D. J. Love, J. V. Krogmeier, T. A. Thomas, and A. Ghosh, "Millimeter wave beamforming for wireless backhaul and access in small cell networks," *IEEE Transactions on Communications*, vol. 61, no. 10, pp. 4391–4403, October 2013.

[20] M. Gapeyenko, A. Samuylov, M. Gerasimenko, D. Moltchanov, S. Singh, E. Aryafar, S. Yeh, N. Himayat, S. Andreev, and Y. Koucheryavy, "Analysis of human body blockage in urban millimeter-wave wireless communications systems," in *2016 IEEE International Conference on Communications*, May 2016.

[21] Y. Zeng, R. Zhang, and T. J. Lim, "Wireless communications with unmanned aerial vehicles: opportunities and challenges," *IEEE Communications Magazine*, vol. 54, no. 5, pp. 36–42, May 2016.

[22] J. G. Andrews, T. Bai, M. Kulkarni, A. Alkhateeb, A. Gupta, and R. W. Heath Jr., "Modeling and analyzing millimeter wave cellular systems," *IEEE Transactions on Communications*, vol. 65, no. 1, pp. 403–430, January 2016.

[23] "MOSEK ApS optimization software," *https://www.mosek.com/*.

[24] R. Webster, *Convexity*. Oxford University Press, 1994.